A&A 518, L84 (2010)
DOI: 10.1051/0004-6361/201014629

Herschel: the first science highlights

Astronomy & Astrophysics
Special feature

Letter to the Editor

Herschel★ observations of embedded protostellar clusters in the Rosette molecular cloud★★

M. Hennemann[1], F. Motte[1], S. Bontemps[1,2], N. Schneider[1], T. Csengeri[1], Z. Balog[3], J. Di Francesco[4], A. Zavagno[5], Ph. André[1], A. Men'shchikov[1], A. Abergel[6], B. Ali[7], J.-P. Baluteau[5], J.-Ph. Bernard[8], P. Cox[9], P. Didelon[1], A.-M. di Giorgio[10], M. Griffin[11], P. Hargrave[11], T. Hill[1], B. Horeau[1], M. Huang[12], J. Kirk[11], S. Leeks[13], J. Z. Li[12], A. Marston[14], P. Martin[15], S. Molinari[10], Q. Nguyen Luong[1], G. Olofsson[16], P. Persi[17], S. Pezzuto[10], D. Russeil[5], P. Saraceno[10], M. Sauvage[1], B. Sibthorpe[18], L. Spinoglio[10], L. Testi[19], D. Ward-Thompson[11], G. White[13,20], C. Wilson[21], and A. Woodcraft[18]

(Affiliations are available in the online edition)

Received 31 March 2010 / Accepted 2 May 2010

ABSTRACT

The *Herschel* OB young stellar objects survey (HOBYS) has observed the Rosette molecular cloud, providing an unprecedented view of its star formation activity. These new far-infrared data reveal a population of compact young stellar objects whose physical properties we aim to characterise. We compiled a sample of protostars and their spectral energy distributions that covers the near-infrared to submillimetre wavelength range. These were used to constrain key properties in the protostellar evolution, bolometric luminosity, and envelope mass and to build an evolutionary diagram. Several clusters are distinguished including the cloud centre, the embedded clusters in the vicinity of luminous infrared sources, and the interaction region. The analysed protostellar population in Rosette ranges from 0.1 to about 15 $M_{\odot}$ with luminosities between 1 and 150 $L_{\odot}$, which extends the evolutionary diagram from low-mass protostars into the high-mass regime. Some sources lack counterparts at near- to mid-infrared wavelengths, indicating extreme youth. The central cluster and the Phelps & Lada 7 cluster appear less evolved than the remainder of the analysed protostellar population. For the central cluster, we find indications that about 25% of the protostars classified as Class I from near- to mid-infrared data are actually candidate Class 0 objects. As a showcase for protostellar evolution, we analysed four protostars of low- to intermediate-mass in a single dense core, and they represent different evolutionary stages from Class 0 to Class I. Their mid- to far-infrared spectral slopes flatten towards the Class I stage, and the 160 to 70 μm flux ratio is greatest for the presumed Class 0 source. This shows that the *Herschel* observations characterise the earliest stages of protostellar evolution in detail.

Key words. stars: formation – stars: protostars – ISM: individual objects: Rosette

1. Introduction

The HOBYS *Herschel* (Pilbratt et al. 2010) imaging survey (Motte et al. 2010) is a key programme for studying the sites of OB star formation within a distance of 3 kpc. The parallel mode scan map observations, carried out with the PACS (Poglitsch et al. 2010) and SPIRE (Griffin et al. 2010; Swinyard et al. 2010) instruments, provide maps of massive cloud complexes in the wavelength range of 70 to 500 μm, and thus a census of the different stages of star formation from prestellar cores to evolved young stellar objects (YSOs). As an excellent example of a massive cloud complex associated with – and under the influence of – an OB star cluster (NGC 2244), the Rosette molecular cloud was observed for HOBYS during the *Herschel* science demonstration phase (Motte et al. 2010). The influence of NGC 2244 on the cloud complex is discussed in the accompanying paper by Schneider et al. (2010), while Di Francesco et al. (2010) assesses the clump population. For consistency with Schneider et al. (2010), the distance of Rosette adopted here is 1.6 kpc. Many previous studies have targeted the Rosette complex. Ongoing star formation across the molecular cloud is traced by the presence of several luminous IRAS sources that are associated with massive clumps seen in CO emission (Cox et al. 1990; Williams et al. 1995; Schneider et al. 1998). Towards these dense regions, the embedded clusters PL1 to PL7 have been identified by Phelps & Lada (1997) from near-infrared observations. The list of clusters in Rosette was extended by Li & Smith (2005), Román-Zúñiga et al. (2008), and Poulton et al. (2008) using near-infrared and *Spitzer* observations.

In this paper, we make use of the unprecedented spatial resolution and sensitivity of *Herschel* to establish a sample of compact far-infrared sources that represent protostellar objects and to determine their fundamental properties (luminosities and envelope masses) from their spectral energy distribution (SED). In the early phases of the collapse of a protostellar core and the initial accretion of matter onto a central protostar, the SED of a Class 0 source is dominated by thermal emission from cold dust in the envelope ($M_{\rm env} > M_{\star}$, André et al. 2000). The SED of a more evolved Class I source is shifted to mid-infrared wavelengths, indicating a comparatively less massive, hotter envelope ($M_{\rm env} < M_{\star}$). To investigate the evolutionary stage,

★ *Herschel* is an ESA space observatory with science instruments provided by European-led Principal Investigator consortia and with important participation from NASA.

★★ Figure 4 is only available in electronic form at http://www.aanda.org the protostellar envelope mass is usually compared to the bolometric luminosity, which serves as a proxy for stellar mass. The *Herschel* observations for the first time cover the peak of the protostellar SED thus constraining the evolutionary stage of early-to-evolved YSOs. This overcomes the previous difficulties distinguishing Class 0 and Class I sources using near- to mid-infrared data.

2. Observations

The Rosette molecular cloud was observed by *Herschel* on October 20, 2009 in the parallel scan map mode (scanning speed of 20″/sec) simultaneously with SPIRE at 250/350/500 μm and PACS at 70/160 μm. Two perpendicular scans (consisting of parallel scanlegs interspersed by turn-arounds) were taken to cover a SPIRE/PACS common area of $1^\circ \times 1^\circ$. The data are reduced with scripts developed in HIPE[1] (Ott 2010, version 2.0 for SPIRE and version 3.0 for PACS). The PACS data are deglitched from cosmic ray impacts with the HIPE second-level method and then high-pass filtered with a scanleg filter width to preserve the extended emission up to the map size scale. The combined scans are finally projected using the HIPE MadMAP implementation with the noise table Invntt version 1. For details of the SPIRE data reduction, see Schneider et al. (2010). The maps are flux-calibrated according to the correction factors of Swinyard et al. (2010) and Poglitsch et al. (2010), compared to 2MASS to correct for a $\sim$6″ pointing offset and a systematic offset of $\sim$4″ between SPIRE and PACS. The entire set of *Herschel* maps is shown in Motte et al. (2010), and Fig. 4 (available online) shows the 70 and 160 μm maps.

3. Results and analysis

Rosette harbours several luminous far-infrared sources that represent candidate high-mass protostars with AFGL 961 being the brightest (see Motte et al. 2010). In their vicinity, the *Herschel* 70 and 160 μm maps reveal a population of compact sources that likely represent YSOs of low to intermediate mass. The most prominent cluster is the one towards the Rosette molecular cloud centre (see Fig. 1). The emission traces heated protostellar envelope material; in contrast, starless cores are not expected to be detected as compact sources at 70 μm. That *Herschel* resolves individual protostars, even though the Rosette region lies at an intermediate distance, allows us to study the physical properties of the protostar population based on unprecedented far-infrared data.

3.1. Identification of compact protostellar sources

To identify the positions of the compact *Herschel* protostars, we made use of the 70 μm *MRE-GCL* catalogue (Motte et al. 2010) derived using the method of Motte et al. (2007). Spatial scales larger than 0.5 pc were filtered out using *MRE* (Starck & Murtagh 2006), and the *Gaussclumps* programme applied (Kramer et al. 1998). We focused on the protostellar objects clearly detected at 70 μm with $FWHM < 15''$ and derived the 70 and 160 μm flux measurements using aperture photometry. Sources that are faint or that appear non-singular, either of which prevents a useful measurement, were excluded. The aperture diameters were chosen to correspond to a physical scale of 0.1 pc (corresponding to a source *FWHM* size of roughly 0.05 pc) and

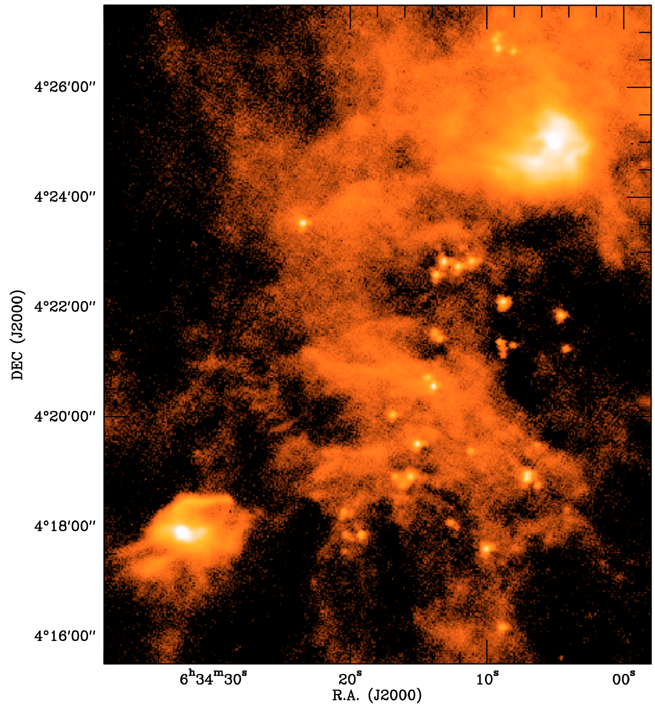

Fig. 1. PACS 70 μm of the Rosette molecular cloud centre. The region harbours the embedded clusters PL4 (northwest), PL5 (southeast), and a concentration of compact *Herschel* sources.

the background is determined in adjacent annuli. Figures 1 and 3 show that protostars are resolved at 70 and 160 μm but blend together in the submillimetre, preventing a dust temperature measurement on the protostar scale. Thus we adopted temperatures determined by Motte et al. (2010) derived from the integrated emission on larger scales, using greybody fits with a dust emissivity index of $\beta = 2$ and assuming $T_\mathrm{d} = 20$ K for sources where no estimate is available. This may introduce a bias towards low temperatures as the protostellar envelopes are expected to be warmer than their surroundings. The envelope masses were estimated by scaling the greybody curve (of dense cores) to the 160 μm fluxes (of protostellar envelopes). Eighty eight protostars are the basis for the further study described below. Due to the compactness criterion, this sample does not include the high-luminosity, high-mass protostellar objects (e.g. AFGL 961).

Partly based on *Spitzer* IRAC and MIPS data of the same region obtained by Poulton et al. (2008) and on 2MASS, a catalogue supplied by Balog et al. (in prep., hereafter referred to as *Spitzer* catalogue) was used to search for source counterparts in the near- and mid-infrared. Considering $\sim$1900 sources catalogued at 24 μm, 17 *Herschel* sources have no counterpart. The inspection of the maps shows that most of them are either not covered by the MIPS observations or are not included in the catalogue owing to artifacts in the *Spitzer* maps. Interestingly, 5 sources have only been detected with *Herschel* but not at 24 μm (completeness limit $\sim$0.5 mJy). The *Spitzer* catalogue also includes a classification of source type using the IRAC colours Gutermuth et al. (2008). The compiled flux measurements that include the *Spitzer* catalogue are used to estimate bolometric luminosities by integration over the SEDs, where we use the submillimetre fluxes of a greybody with the adopted dust temperature. The current lack of resolved submillimetre flux measurements means that the mass derivation relies on assumptions of the dust temperature and emissivity, and we estimate that the relative accuracy is roughly a factor of 2, and similarly for the luminosities. This will be improved by forthcoming studies.

[1] HIPE is a joint development by the *Herschel* Science Ground Segment Consortium, consisting of ESA, the NASA *Herschel* Science Center, and the HIFI, PACS, and SPIRE consortia.

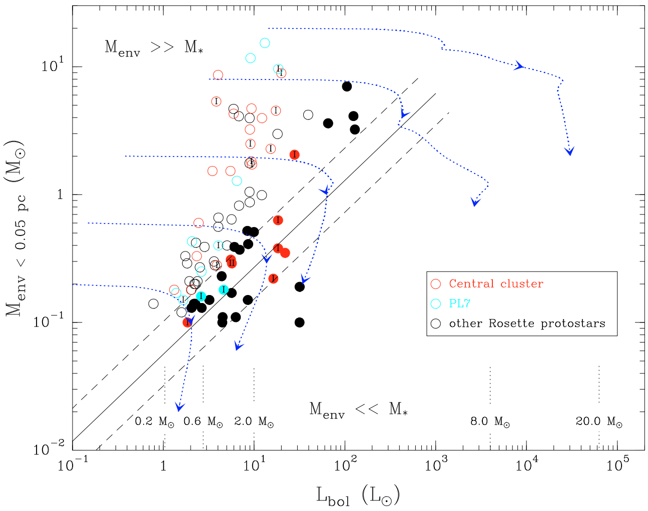

Fig. 2. Envelope mass versus bolometric luminosity diagram for the sample of *Herschel* protostars in Rosette. Evolutionary tracks for stellar masses between 0.2 and 20 $M_\odot$ are included. The solid line corresponds to 50% of the mass accreted; the dashed lines account for the estimated uncertainties of $M_{\rm env}$ and $L_{\rm bol}$. Open symbols: candidate Class 0 protostars with $L_{\lambda>350\,\mu{\rm m}}/L_{\rm bol} > 1\%$; filled symbols: Class I protostars with $L_{\lambda>350\,\mu{\rm m}}/L_{\rm bol} \leq 1\%$.

3.2. Evolutionary stage of the Herschel protostars in Rosette

The derived envelope masses and bolometric luminosities are plotted in an evolutionary diagram shown in Fig. 2. For clarity, we omit the aforementioned error estimates. Such a diagram is proposed to trace the evolution of embedded protostars (Bontemps et al. 1996; Saraceno et al. 1996) because Class 0 sources display relatively high envelope masses that decrease during the mass accretion, while the luminosities (protostellar core and accretion) increase significantly. Evolutionary tracks are displayed for stars of different masses (cf. André et al. 2008; Bontemps et al. 2010). The Rosette protostar sample occupies the low- to high-mass regimes in the diagram. Compared to findings in the nearby Aquila star-forming region (Bontemps et al. 2010), the Rosette protostars are comprised of higher masses. The diagonal lines in Fig. 2 (see caption) indicate an approximate border zone between envelope-dominated Class 0 and star-dominated Class I objects based on the comparison of $M_{\rm env}$ to $M_\star$ (cf. André & Montmerle 1994).

A surprisingly large fraction of our sample (~2/3) falls into the candidate Class 0 regime above these lines. A practical criterion inferred from this diagram is $L_{\lambda>350\,\mu{\rm m}}/L_{\rm bol} > 1\%$ for Class 0 (André et al. 2000). In Fig. 2 we apply this criterion obtained from the previously compiled SEDs. It results in more intermediate-mass objects being classified as Class I, i.e., a more conservative Class 0 assignment that we hereafter refer to as "candidate Class 0". The classification of objects lying near the border zone remains tentative because of the uncertainty in converting the $M_{\rm env}/M_\star$ ratio into measurable quantities. In particular, the *Herschel* photometry of nearby protostars will reduce this uncertainty, after data from several regions have been analysed. Until a detailed analysis of the completeness is available, our finding thus remains preliminary. Nevertheless, it indicates that *Herschel* allows us to significantly extend the sample of known Class 0 objects.

Seven protostar subsamples are established according to their location (field denominations in Schneider et al. 2010), which are listed in Table 1. The distributed protostars contains sources located towards the tip of pillar structures (Schneider et al. 2010). Each subsample spans a wide mass range from 0.1 to about 10 $M_\odot$. In Fig. 2 the central cluster and PL7 subsamples are emphasised by coloured symbols. In the 2 to 10 $M_\odot$ range, the central cluster harbours a significant number of sources in the Class 0 regime with 4 to 30 $L_\odot$. Also the PL7 cluster contains 3 sources with relatively low luminosities. This indicates that both the central cluster and the PL7 cluster are younger compared to the remaining protostars.

Table 1. Protostar subsamples seen by *Herschel* in Rosette.

Region	Associated Clusters	# Protostars
Centre	PL4/5, REFL08, E	27
Shell	PL1, A	5
Monoceros Ridge/ Extended Ridge	PL2, C	11
PL3	–	4
AFGL 961	PL6	6
PL7	G	11
Distributed	–	24

Notes. Cluster names are PL for Phelps & Lada (1997), REFL for Román-Zúñiga et al. (2008), A…G for Poulton et al. (2008).

Table 2. Classification of protostars in the Rosette central cluster.

	# total	# Class II	# Class I	# Unclass.
24 μm sources	83	39	26	18
Visible in 70 μm	40 (±3)	10 (±1)	19 (±1)	11 (±1)
In *Herschel* sample	22	1	12	9
Candidate Class 0	14	0	7	7

Notes. The cluster area is defined here by 98.5° < RA < 98.6° and 4.25° < Dec < 4.4°. The table head classifications base on near- to mid-infrared measurements. Class 0 candidates exhibit $L_{\lambda>350\,\mu{\rm m}}/L_{\rm bol} > 1\%$.

3.3. The classification of protostars in the central cluster

Among the 27 *Herschel* protostars in our central cluster sample, the *Spitzer* classification (see Sect. 3.1) gives 12 Class I objects and one for Class II. For PL7, 5 out of 11 sources are classified as Class I. These classifications are added to the symbols in Fig. 2 as "I" and "II", for comparison to their location in the evolutionary diagram and the distinction by the $L_{\lambda>350\,\mu{\rm m}}/L_{\rm bol}$ ratio. Notably, about half of the sources seen as Class I by *Spitzer* in these two subsamples correspond to sources with $L_{\lambda>350\,\mu{\rm m}}/L_{\rm bol} > 1\%$ and thus represent candidate Class 0 protostars. They are intermixed with the unclassified sources in the diagram that lack detections in one or several bands. This suggests that the classification based on the near- to mid-infrared data alone has to be partly revised in light of the *Herschel* measurement of the protostellar envelope.

To overcome incompleteness in our *Herschel* catalogue and to provide a first census of how many sources classified using near- to mid-infrared data are affected, we have focused on the central cluster. We redefined the cluster area as a rectangular field towards the Rosette molecular cloud centre and selected a total of 86 catalogued 24 μm sources in that field. Three 24 μm sources were classified as probably extragalactic and are excluded. We then inspected the *Herschel* 70 μm map for counterparts. The field and the resulting detection statistics are given in Table 2. The chosen field excludes PL4 and its vicinity because the extended emission there makes source identification very uncertain. Still there is a bias towards bright objects, and we estimate an uncertainty of three sources in total and one source per subsample. Based on visual inspection, we find a 70 μm detection rate of about 50% for YSOs seen at 24 μm.

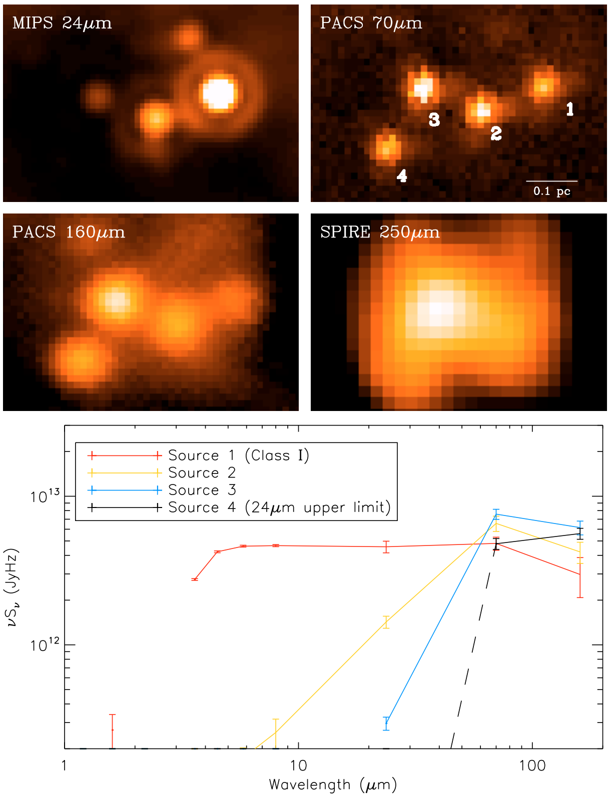

Fig. 3. Four protostars in the central cluster at 24, 70, 160, and 250 μm and their spectral energy distributions.

Due to their rising SED, we expect more 70 μm detections for Class I than for Class II, and find about 3/4 compared to about 1/4. In the second row of Table 2, we list the corresponding numbers for the analysed *Herschel* sample and the classification for the same field. Roughly, we include about half of the visible 70 μm sources in the *Herschel* list. About 2/3 of these are Class 0 candidates. This applies to 7 out of 18 unclassified sources, which indicates that many of the latter are Class 0 protostars. About 25% of 26 previously classified Class I sources are also Class 0 candidates, possibly more. Notably, our statistical basis is low and will be improved in forthcoming studies.

For illustration, we consider a particularly interesting large dense core revealed by *Herschel* which is resolved into several protostars at 70/160 μm (Fig. 3). For the whole core, Motte et al. (2010) derive a dust temperature of 15 K. We focus on 4 sources clearly detected at 70 μm labelled 1 to 4 from west to east. The projected separation between two neighbours is around 0.14 pc. At 24 μm, only sources 1 to 3 are detected with decreasing brightness. Based on the *Spitzer* data, source 1 is classified as Class I, while the others remain unclassified owing to non-detection in one or more of the IRAC bands (sources 2 and 3) or non-detection in all near- to mid-infrared bands (source 4). At 70 and 160 μm source 4 shows up and the adjacent source 3 is the brightest of the group. The SED slopes (Fig. 3) between 8 and 70 μm for sources 1, 2, and 3 become increasingly steep. Beyond 70 μm they are shallower, and the 160 to 70 μm flux ratio is the highest for source 4. The mid- to far-infrared colours allow us to distinguish the source evolutionary stages.

The derived luminosities ($M_{\rm env}^{<0.05\,\rm pc}$, $L_{\lambda\,>\,350\,\mu\rm m}/L_{\rm bol}$) are 15 $L_\odot$ (2 $M_\odot$, 1%) for source 1, 8 $L_\odot$ (3 $M_\odot$, 3%) for source 2, 8 $L_\odot$ (5 $M_\odot$, 4%) for source 3, and 5 $L_\odot$ (4 $M_\odot$, 6%) for source 4. We note that the assumption of a single dust temperature means the relative mass differences are not well constrained. Relatively similar in mass, the sources represent successive evolutionary stages from early Class 0 (source 4) to "flat-spectrum" Class I (source 1). This is a first example of how *Herschel* resolves the early evolution of protostars in combination with *Spitzer* measurements.

4. Implications

This initial study of the protostellar population in Rosette using the HOBYS observations already shows that *Herschel* provides detailed insight into the earliest stages of the protostellar evolution at low to high masses, and in particular identifies thus far elusive Class 0 objects. The now available *Herschel* photometry will be the basis for establishing firm criteria (mid- to far-infrared colours) for distinguishing the evolutionary stages, including the observations of nearby regions where individual (low-mass) protostars are resolved in the submillimetre. Based on a complete protostar catalogue of the Rosette complex, we will examine the evolution of the star formation activity over the whole cloud also with respect to triggering (cf. Schneider et al. 2010).

Acknowledgements. SPIRE has been developed by a consortium of institutes led by Cardiff Univ. (UK) and including Univ. Lethbridge (Canada); NAOC (China); CEA, LAM (France); IFSI, Univ. Padua (Italy); IAC (Spain); Stockholm Observatory (Sweden); Imperial College London, RAL, UCL-MSSL, UKATC, Univ. Sussex (UK); Caltech, JPL, NHSC, Univ. Colorado (USA). This development has been supported by national funding agencies: CSA (Canada); NAOC (China); CEA, CNES, CNRS (France); ASI (Italy); MCINN (Spain); SNSB (Sweden); STFC (UK); and NASA (USA). PACS has been developed by a consortium of institutes led by MPE (Germany) and including UVIE (Austria); KU Leuven, CSL, IMEC (Belgium); CEA, LAM (France); MPIA (Germany); INAF-IFSI/OAA/OAP/OAT, LENS, SISSA (Italy); IAC (Spain). This development has been supported by the funding agencies BMVIT (Austria), ESA-PRODEX (Belgium), CEA/CNES (France), DLR (Germany), ASI/INAF (Italy), and CICYT/MCYT (Spain). Part of this work was supported by the ANR (*Agence Nationale pour la Recherche*) project "PROBeS", number ANR-08-BLAN-0241. We thank the anonymous referee for helpful comments.

References

André, P., & Montmerle, T. 1994, ApJ, 420, 837
André, P., et al. 2000, Protostars and Planets IV, 59
André, P., Minier, V., Gallais, P., et al. 2008, A&A, 490, L27
Bontemps, S., Andre, P., Terebey, S., & Cabrit, S. 1996, A&A, 311, 858
Bontemps, S., et al. 2010, A&A, 518, L85
Cox, P., Deharveng, L., & Leene, A. 1990, A&A, 230, 181
Di Francesco, J., et al. 2010, A&A, 518, L91
Griffin, M. J., et al. 2010, A&A, 518, L3
Gutermuth, R. A., Myers, P. C., Megeath, S. T., et al. 2008, ApJ, 674, 336
Kramer, C., Stutzki, J., Rohrig, R., & Corneliussen, U. 1998, A&A, 329, 249
Li, J. Z., & Smith, M. D. 2005, ApJ, 620, 816
Motte, F., Bontemps, S., Schilke, P., et al. 2007, A&A, 476, 1243
Motte, F., et al. 2010, A&A, 518, L77
Ott, S. 2010, in Astronomical Data Analysis Software and Systems XIX, ed. Y. Mizumoto, K.-I. Morita, & M. Ohishi, ASP Conf. Ser., in press
Phelps, R. L., & Lada, E. A. 1997, ApJ, 477, 176
Pilbratt, G. L., et al. 2010, A&A, 518, L1
Poglitsch, A., et al. 2010, A&A, 518, L2
Poulton, C. J., Robitaille, T. P., Greaves, J. S., et al. 2008, MNRAS, 384, 1249
Román-Zúñiga, C. G., Elston, R., et al. 2008, ApJ, 672, 861
Saraceno, P., Andre, P., Ceccarelli, C., et al. 1996, A&A, 309, 827
Schneider, N., Stutzki, J., Winnewisser, G., & Block, D. 1998, A&A, 335, 1049
Schneider, N., et al. 2010, A&A, 518, L83
Starck, J., & Murtagh, F. 2006, Astronomical Image and Data Analysis, ed. J.-L. Starck, & F. Murtagh
Swinyard, B. M., et al. 2010, A&A, 518, L4
Williams, J. P., Blitz, L., & Stark, A. A. 1995, ApJ, 451, 252

Page 5 is available in the electronic edition of the journal at `http://www.aanda.org`

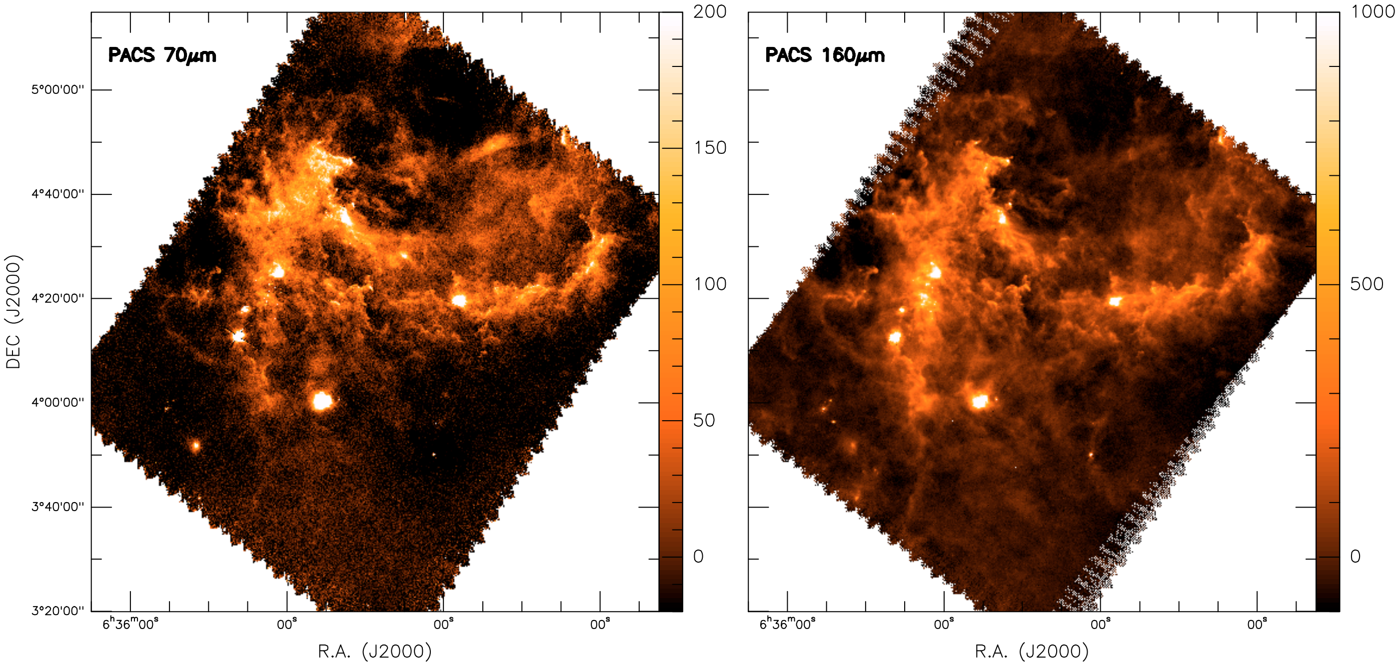

Fig. 4. HOBYS *Herschel* 70 and 160 μm maps of the Rosette molecular cloud (flux unit: MJy/sr). See Motte et al. (2010) for details on the sensitivity of the entire *Herschel* data set.

[1] Laboratoire AIM, CEA/IRFU – CNRS/INSU – Université Paris Diderot, CEA-Saclay, 91191 Gif-sur-Yvette Cedex, France
e-mail: `martin.hennemann@cea.fr`

[2] Laboratoire d'Astrophysique de Bordeaux, CNRS/INSU – Université de Bordeaux, BP 89, 33271 Floirac Cedex, France

[3] Max-Planck-Institut für Astronomie, Königstuhl 17, Heidelberg, Germany

[4] National Research Council of Canada, Herzberg Institute of Astrophysics, University of Victoria, Department of Physics and Astronomy, Victoria, Canada

[5] Laboratoire d'Astrophysique de Marseille, CNRS/INSU – Université de Provence, 13388 Marseille Cedex 13, France

[6] IAS, Université Paris-Sud, 91435 Orsay, France

[7] NHSC/IPAC, California Institute of Technology, Pasadena, CA, USA

[8] CESR & UMR 5187 du CNRS/Université de Toulouse, BP 4346, 31028 Toulouse Cedex 4, France

[9] IRAM, 300 rue de la Piscine, Domaine Universitaire, 38406 Saint-Martin-d'Hères, France

[10] INAF-IFSI, Fosso del Cavaliere 100, 00133 Roma, Italy

[11] Cardiff University School of Physics and Astronomy, UK

[12] National Astronomical Observatories, Chinese Academy of Sciences, Beijing 100012, PR China

[13] Space Science and Technology Department, Rutherford Appleton Laboratory, Chilton, Didcot OX11 0NL, UK

[14] Herschel Science Centre, ESAC, ESA, PO Box 78, Villanueva de la Cañada, 28691 Madrid, Spain

[15] CITA & Dep. of Astronomy and Astrophysics, University of Toronto, Toronto, Canada

[16] Department of Astronomy, Stockholm University, AlbaNova University Center, Roslagstullsbacken 21, 10691 Stockholm, Sweden

[17] INAF-IASF, Sez. di Roma, via Fosso del Cavaliere 100, 00133 Roma, Italy

[18] UK Astronomy Technology Centre, Royal Observatory Edinburgh, Blackford Hill, EH9 3HJ, UK

[19] ESO, Karl Schwarzschild Str. 2, 85748 Garching, Germany

[20] Department of Physics & Astronomy, The Open University, Milton Keynes MK7 6AA, UK

[21] McMaster University, Hamilton, Canada